+ MODEL

Available online at www.sciencedirect.com

ScienceDirect

Publishing Services by Elsevier

International Journal of Naval Architecture and Ocean Engineering xx (2016) 1–10

http://www.journals.elsevier.com/international-journal-of-naval-architecture-and-ocean-engineering/

Hydrodynamics of single-deadrise hulls and their catamaran configurations

Ghazi S. Bari, Konstantin I. Matveev*

School of Mechanical and Materials Engineering, Washington State University, Pullman, WA 99164-2920, USA

Received 12 September 2016; revised 21 October 2016; accepted 8 November 2016

Available online ■ ■ ■

Abstract

Asymmetric planing hulls are often used on high-speed catamarans. In this study, a linearized potential-flow method is applied for modeling steady hydrodynamics of single asymmetric hulls and their catamaran setups. Numerical results are validated with available experimental data and empirical correlations. Parametric calculation results are presented for the lift coefficient and the center of pressure for variable hull geometry, spacings, and speed regimes. The lift coefficient is found to increase at smaller hull spacings and decrease at higher Froude numbers and higher deadrise angles.

Keywords: Asymmetric hulls; Planing; Catamarans; Numerical modeling; Potential flow

1. Introduction

Fast boats often employ hard-chine hulls that allow them to skim on the water surface at high speeds. This motion regime, when hydrodynamic lift becomes important and sometimes dominant, is known as planing. It usually occurs when a displacement Froude number exceeds three or a length Froude number is greater than one. To improve roll stability of planing boats and to increase their deck space, twin-hull arrangements are often implemented. In such catamaran configurations, hulls can be made either symmetrical or asymmetrical. In the symmetrical option, the individual drag of each hull is generally lower. However, asymmetrical setups can reduce hydrodynamic interference between hulls, decrease spray impinging on the bottom of the platform between hulls, and provide a more convenient arrangement for installing hydrofoils (Migeotte, 2002).

The present paper focuses on steady hydrodynamic modeling of single-deadrise hulls (one common type of asymmetrical hulls) and their catamaran arrangements in semi-planing and early planing regimes. Fig. 1a shows a general schematic of one catamaran of this kind, and a cross-section of a *single* asymmetric hull is given in Fig. 1b. The most common arrangement of single-deadrise hulls in a twin-hull configuration is shown in Fig. 1c (it will be called a "normal" setup for the rest of the paper). Occasionally, hulls with inverted deadrise are employed (Fig. 1d); below it will be referred to as an "inverted" setup.

Experiments with inclined flat plates similar to single-deadrise hulls were conducted by Savitsky et al. (1958) at very high Froude numbers, applicable for water-based aircraft. More recently, individual single-deadrise hulls were tested by Morabito (2011) at moderate Froude numbers, corresponding to planing boats. Of some relevance to this paper's topic are also studies done by Judge (2013) on heeled planing hulls in relation to roll stability. A discussion on single-deadrise hull design was given by Payne (1988).

Empirical correlations for hydrodynamic interference effects on hulls of planing catamarans were suggested by Savitsky and Dingee (1954) at very high Froude numbers and by Liu and Wang (1979) and Lee (1982) at moderate Froude numbers. The potential-flow modeling of planing catamarans with *symmetrical* hulls was recently carried out by Bari and Matveev (2016). In the literature, one can also find more

* Corresponding author.
E-mail address: matveev@wsu.edu (K.I. Matveev).

Peer review under responsibility of Society of Naval Architects of Korea.

http://dx.doi.org/10.1016/j.ijnaoe.2016.11.001

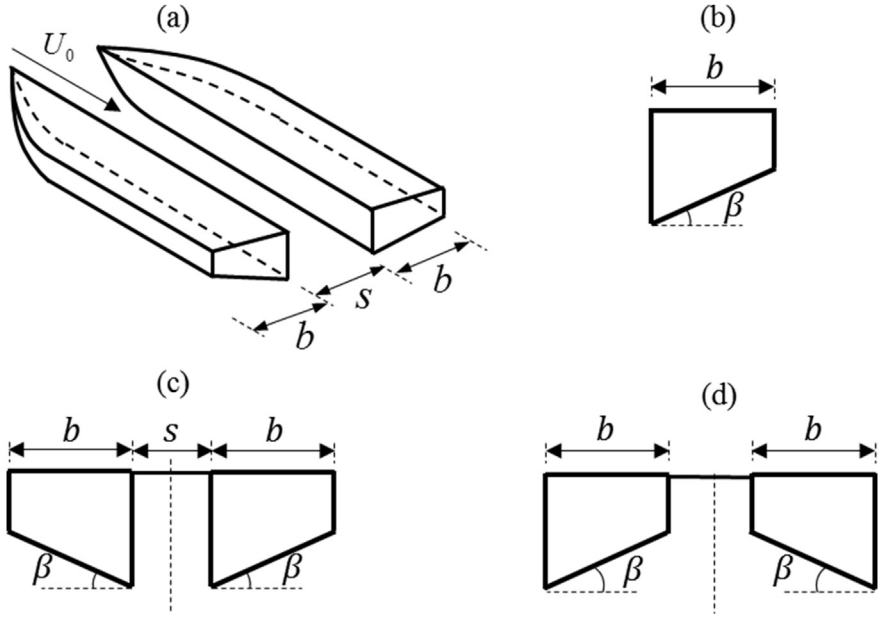

Fig. 1. (a) Schematic of a catamaran with single-deadrise hulls. Cross-sections of (b) one single-deadrise hull, (c) normal twin-hull setup, and (d) inverse twin-hull setup.

detailed (and computationally expensive) CFD studies of specific cases of high-speed multi-hulls (e.g., Zhou, 2003; Kandasamy et al., 2011; Yousefi et al., 2014).

The numerical method employed in this study is based on a linearized potential flow theory with hydrodynamic singularities of a source type distributed on the water surface. This approach was previously developed and validated for conventional planing hulls (Matveev and Ockfen, 2009; Matveev, 2014a), air-cavity hulls (Matveev and Miller, 2011), and air-supported marine craft (Matveev, 2014b). The current method belongs to a class of boundary element methods which are often used for modeling high-speed hulls (e.g., Doctors, 1974; Lai and Troesch, 1996; Benedict et al., 2002). For a descriptive list of other modeling techniques applied in planing hydrodynamics, one can refer to a review by Yousefi et al. (2013).

2. Mathematical model

In flows with high Reynolds number, viscous forces are often negligible outside of thin boundary layers near solid surfaces and separation zones behind blunt bodies. To calculate pressure distribution on a planing hull that disturbs water relatively weakly, the water flow in the present method is assumed to be inviscid, irrotational, incompressible and steady. A general schematic for the numerical model is given in Fig. 2. The boat hull is assumed to be stationary, whereas the water flows from left to right. A potential-flow method based on the point sources positioned on the water surface is utilized here to study to hydrodynamics of single-deadrise hulls and their catamaran setups. The water flow is assumed to be symmetric with respect to the catamaran center plane ($z = 0$), which allows us to use mirror source images on the port side of the numerical domain and reduce the number of unknown variables. In the case of a single hull (Fig. 1b), there are no mirror images. Also, effects of a propulsor and airflow are ignored, and only the calm water condition is considered. The water flow is uniform at far upstream with incident flow velocity U_0.

The Bernoulli equation can be applied to the water surface as the dynamic boundary condition,

$$p_0 + \frac{1}{2}\rho U_0^2 = p_w + \frac{1}{2}\rho U_w^2 + \rho g y_w, \tag{1}$$

where p_0 and U_0 are the pressure and velocity in the water flow far upstream of the hull at $y = 0$ (undisturbed water surface), ρ is the water density, and $p_w(x,z)$ and $U_w(x,z)$ are the pressure and velocity on the water surface with elevation $y_w(x,z)$. Assuming small angles of the hull trim and sufficiently high speeds of the water, flow perturbations induced by the hull can be considered small. Hence, the wave slopes and the x-axis velocity perturbation $u' = U_x - U_0$ will also be small. Then, the linearized Bernoulli equation on the water surface can be written as follows,

$$\frac{1}{2}C_p + \frac{u'}{U_0} + 2\pi\frac{y_w}{\lambda} = 0, \tag{2}$$

where $C_p = (p_w - p_0)/(\rho U_0^2/2)$ is the pressure coefficient (zero on the free water surface and non-zero on the wetted hull surface) and $\lambda = 2\pi U_0^2/g$ is the standard length of a wave propagating on the free water surface.

The water flow disturbances induced by the hull are modeled in this study with a distribution of hydrodynamic sources on a horizontal plane at $y = 0$ (Fig. 2). The sources are placed along horizontal lines parallel to the hull chines. A velocity potential of each source fulfills the Laplace equation in the water domain. Eq. (2) is satisfied at the collocation

Please cite this article in press as: Bari, G.S., Matveev, K.I., Hydrodynamics of single-deadrise hulls and their catamaran configurations, International Journal of Naval Architecture and Ocean Engineering (2016), http://dx.doi.org/10.1016/j.ijnaoe.2016.11.001

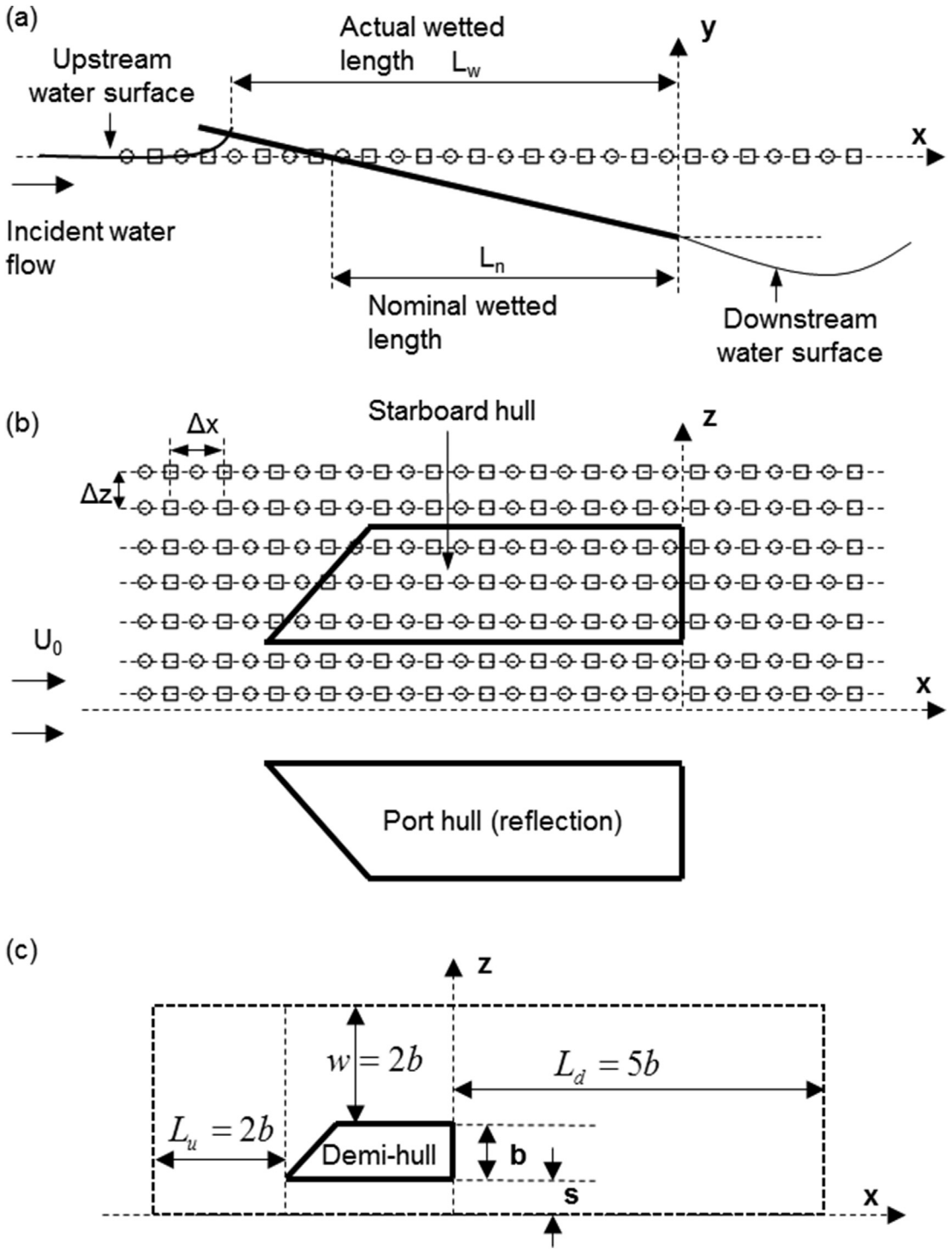

Fig. 2. Geometrical schematic for the computational model. (a) Side view of a longitudinal section, (b) top view of a catamaran setup. Sources and collocation points are shown by circles and squares, respectively. Only small parts of the numerical domain are shown. Distances between sources are exaggerated. (c) Numerical domain of the starboard side of a catamaran with main dimensions; x-axis is the symmetry line.

points that are shifted upstream of the sources by a half distance between neighboring sources (Fig. 2). The staggered arrangement of the sources and collocation points suppresses the wave reflection from the downstream domain boundary (Bertram, 2000). In this approach, the x-component of the velocity perturbation can be computed from the source strengths as follows,

$$u'\left(x_i^c, z_i^c\right) = \frac{1}{4\pi}\sum_j q_j\left(x_i^c - x_j^s\right)\left(\frac{1}{r_{i,j}^3} + \frac{1}{R_{i,j}^3}\right), \tag{3}$$

where $\left(x_i^c, z_i^c\right)$ and $\left(x_j^s, z_j^s\right)$ are the coordinates of the collocation point i and the source j with intensity q_j in the starboard part of the numerical domain, $r_{i,j} = \sqrt{\left(x_i^c - x_j^s\right)^2 + \left(z_i^c - z_j^s\right)^2}$

Please cite this article in press as: Bari, G.S., Matveev, K.I., Hydrodynamics of single-deadrise hulls and their catamaran configurations, International Journal of Naval Architecture and Ocean Engineering (2016), http://dx.doi.org/10.1016/j.ijnaoe.2016.11.001

is the horizontal distance between these points, and $R_{i,j} = \sqrt{(x_i^c - x_j^s)^2 + (z_i^c + z_j^s)^2}$ is the distance between a considered collocation point and the mirror reflection of the source j (with respect to $z = 0$ plane).

The linearized kinematic boundary condition on the water surface relates the source intensities and the local water surface slope, ensuring that there is no flow across this surface (Matveev, 2014b),

$$\frac{1}{2}\left(\frac{q_{i-1}}{\Delta x_{i-1}\Delta z_{i-1}} + \frac{q_i}{\Delta x_i \Delta z_i}\right) = -2U_0 \frac{y_i^s - y_{i-1}^s}{x_i^s - x_{i-1}^s}, \tag{4}$$

where q_{i-1} and q_i are the strengths of the upstream and downstream sources near the collocation point i, Δx and Δz are the intervals between the source locations in x and z directions. In the numerical implementation Δx is kept nearly the same in the hull region, and away from the hull Δx gradually increases with a factor of 1.01 (between two neighboring cells); but its maximal value is capped at $\lambda/30$. Δz stays constant for all cells. On the wetted hull surface, the water surface slope is known, so the strengths of source in that region can be directly related to the hull trim angle τ as $q_i = 2U_0\tau\,\Delta x_i \Delta z_i$. Thus, the linear system of equations (Eqs. (2)–(4)) is formed for the water surface elevations outside the hull, pressure coefficients on the hull surface in contact with water, source intensities, and velocity perturbations. Upon solving this system, one can determine the lift coefficient on the hull and the corresponding center of pressure (from the transom towards the bow) by integrating the pressure coefficient C_p on the hull wetted surface A,

$$C_L = \cos\beta \frac{1}{b^2}\int_A C_P dA, \tag{5}$$

$$L_P = -\frac{\int_A C_P x dA}{\int_A C_P dA}. \tag{6}$$

A specific feature of the considered model is the initially unknown wetted area of the hull since the water tends to rise in front of the planing surfaces (Fig. 2a). The water jet that usually appears near the impingement point on the planing surface is neglected here similar to Riabouchinsky model often applied for developed cavitating flows (Knapp et al., 1970). An iterative numerical procedure is followed to find the actual wetted lengths of the planing hull, $L_w(z)$, since this function is not exactly known in advance. Fig. 3 gives an idea on how the final wetted length of the hull is determined. The front point at each longitudinal section can be initially selected at the intersection of the undisturbed water level and the hull surface, i.e., the wetted length is initially selected as the nominal wetted length, L_n. A water rise can then be calculated after finding a solution to the system of equations with this wetted length. A new intersection of the computed water surface with the hull is then taken as a second guess for defining the wetted length (Fig. 3), and the calculation process is repeated until the location of the front wetted point converges.

The calculation procedure described here is applicable for a hull with assigned trim and sinkage. However, in practical design these parameters are usually unknown in advance. Instead, the hull weight and the center of gravity are commonly specified. In such a case, one needs to use an iterative procedure. Initially, some values for the trim and sinkage can be guessed. If the lift is found to be smaller than the weight, the sinkage should be increased in the next iteration. If the center of pressure appears behind the center of gravity, the trim should be reduced. Upon several iterations, one can determine the equilibrium values for the trim and sinkage, at which the lift is balanced by the weight and the center of pressure is located under the center of gravity.

The mesh-independence studies were conducted in this study for asymmetric catamaran configurations, and the calculated lift slope for one typical setup is shown in Fig. 4 as a function of mesh parameters. These results suggest that the mesh cell size (distance between sources) can be selected as $b/6$ (where b is the demi-hull width). The upstream and side boundaries of the numerical domain can be placed at the distance $2b$ from the hull bow and side, respectively, and the downstream domain boundary should be located at the distance of $5b$ from the hull stern (Fig. 2c). Using bigger numerical domain or finer mesh does not lead to significant variations in the results. A number of sources used in the present calculations usually stays within 2000.

3. Results and discussion

The present numerical method has been previously validated against flat and double-deadrise hulls in early planing regimes (Matveev and Ockfen, 2009; Matveev, 2014a), as well as for air-ventilated underwater surfaces (Matveev, 2003). Morabito (2011) presented experimental results for the lift coefficient of single asymmetric hulls (Fig. 1b) as a function of speed, trim angle, deadrise angle, and mean wetted length-to-beam ratio. Fig. 5 shows a comparison between results of the current numerical model and those test results. The experimental results are given by Morabito (2011) for dispersed values of primary parameters rather than fixed values, although the variations are not extreme. In the set of data used here, the beam Froude number varied in ranges 2.73–2.75 and 3.95–4.01 whereas the trim angle ranged from 5.89° to 6.14°. The beam based Froude number is defined as $Fr = U_0/\sqrt{gb}$, where U_0 is the free steam velocity, g is the gravitational acceleration, and b is the width of the hull. The average values from the given set of Froude numbers and trim angles were used in the present numerical study to compare with experimental findings.

The lift coefficients with respect to the normalized wetted lengths at keel are presented at two speed regimes ($Fr = 2.74$, 3.96) for deadrise angle $\beta = 18°$ and trim angle $\tau = 6°$ in the numerical study. The wetted lengths at keel (L_K) for test data

Please cite this article in press as: Bari, G.S., Matveev, K.I., Hydrodynamics of single-deadrise hulls and their catamaran configurations, International Journal of Naval Architecture and Ocean Engineering (2016), http://dx.doi.org/10.1016/j.ijnaoe.2016.11.001

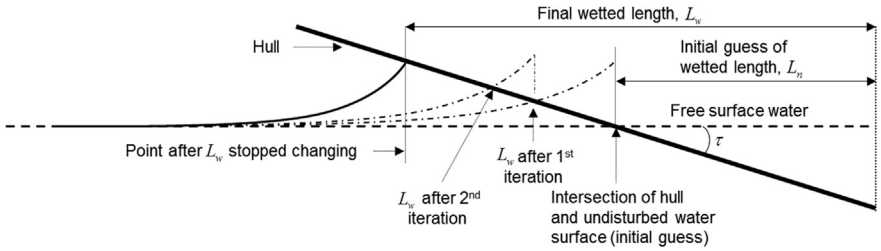

Fig. 3. Iterative process of finding the wetted length on a hull longitudinal section.

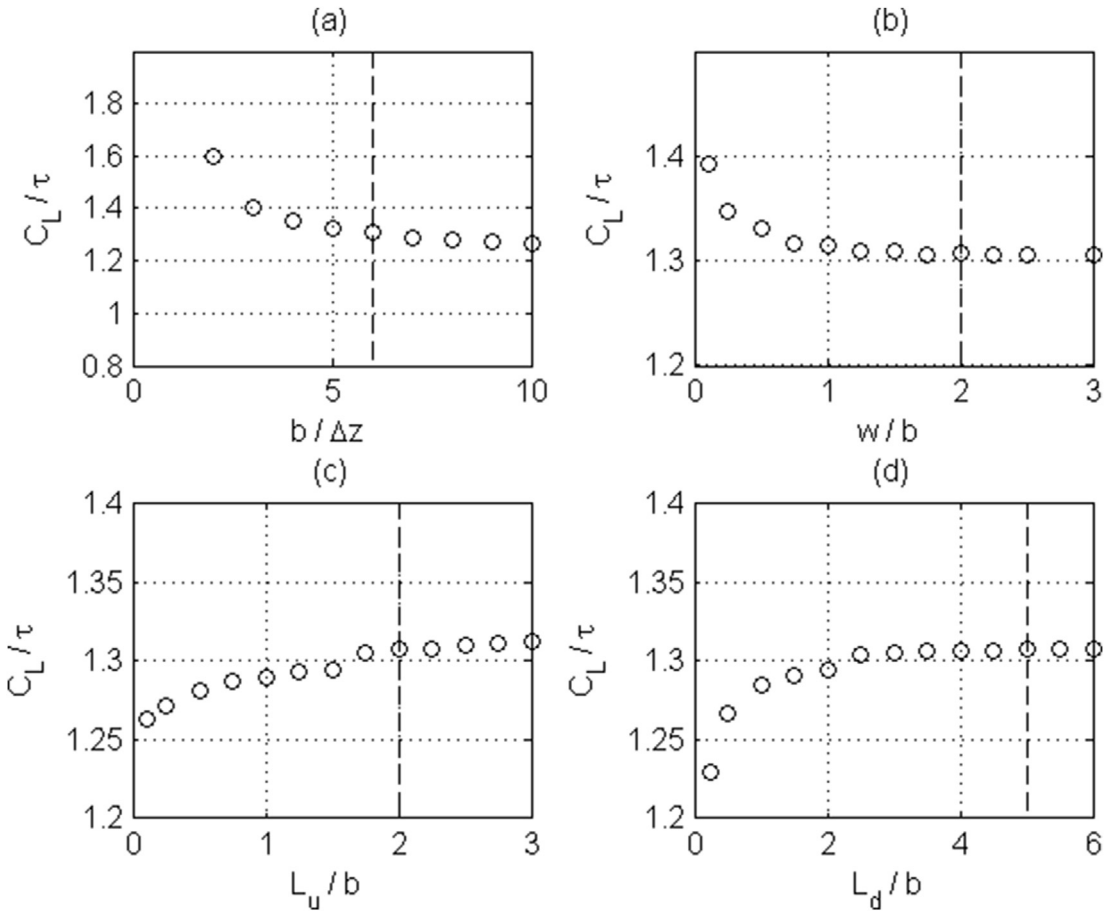

Fig. 4. Variation of lift slope with respect to (a) number of points along the hull beam ($N_h = b/\Delta z$), (b) width of the side domain, (c) length of upstream domain, and (d) length of downstream domain. Vertical lines indicate parameters of the numerical domain used in the following calculations.

are calculated from the reported mean wetted length-to-beam ratio (λ) using the equation $L_K = \lambda b + \frac{b}{\pi}\frac{\tan\beta}{\tan\tau}$ given by Morabito (2011). The trends between numerical and experimental results in Fig. 5 are consistent and reasonably close.

The current numerical model was further validated against an empirical equation for hard-chine catamarans proposed by Liu and Wang (1979). They incorporated a hydrodynamic interference factor due to the spacing between two demi-hulls in the empirical equation by Savitsky (1964) for calculating the lift coefficient. It should be noted that the wetted length used in that empirical equation (Liu and Wang, 1979) is adjusted using another empirical correlation for the wetted length on hydrodynamically interacting hulls given by Savitsky and Dingee (1954). A comparison with the present numerical model is shown in Fig. 6 for a catamaran with the normal hull setup (Fig. 1c) moving at the beam-based Froude number $Fr = 3$ with the mean wetted length-to-beam ratio $\lambda = 3$, deadrise angle $\beta = 18°$, and trim angle $\tau = 6°$. Results of parametric calculations are presented in Fig. 6 for a planing asymmetric catamaran configuration in the form of a correction C_L/C_{L_∞} to the lift coefficient for hulls operating in the catamaran mode, C_L, with respect to a single hull without any interference effects, C_{L_∞}.

Another comparison has been carried out for the shape of the wake behind a flat planing plate. The semi-empirical correlation suggested by Epstein (1969) and more advanced theory of Payne (1984) have previously demonstrated an approximate agreement with available test data. The centerline

Please cite this article in press as: Bari, G.S., Matveev, K.I., Hydrodynamics of single-deadrise hulls and their catamaran configurations, International Journal of Naval Architecture and Ocean Engineering (2016), http://dx.doi.org/10.1016/j.ijnaoe.2016.11.001

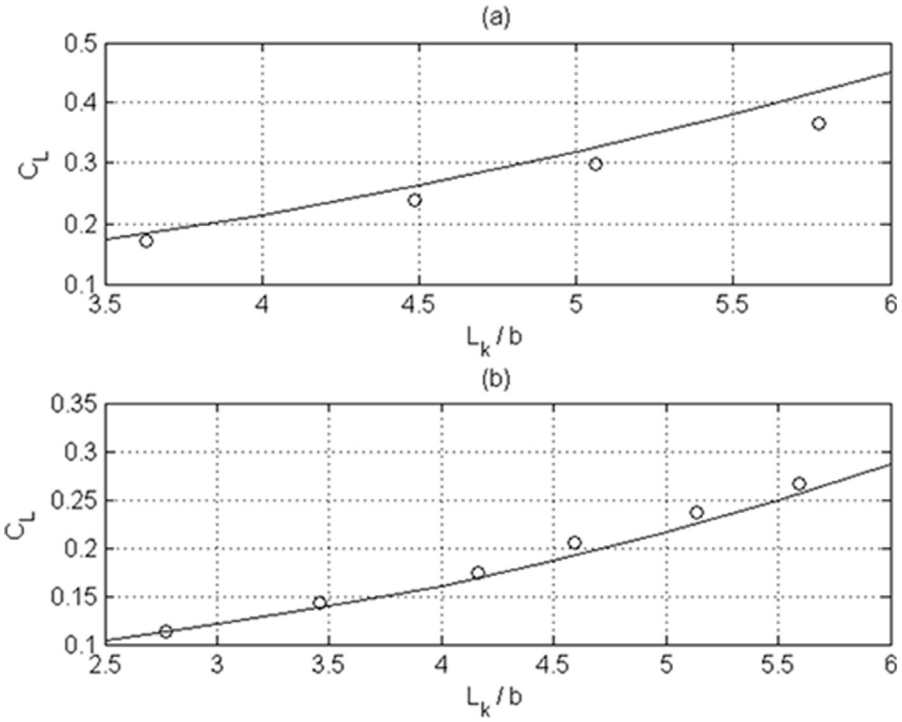

Fig. 5. Comparison of lift coefficients calculated with the present numerical model (lines) and obtained experimentally (circles). (a) $Fr = 2.74$, (b) $Fr = 3.96$.

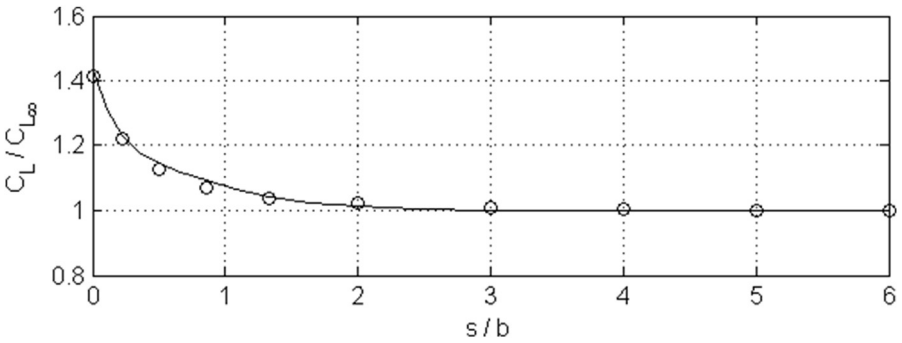

Fig. 6. Comparison of lift coefficients calculated with the present numerical model (circles) and empirical correlation (line).

wake profile was calculated with the present numerical method behind a flat plate planing at the trim angle of 6° with a nominal wetted length of 3 for two Froude numbers (5 and 10). A comparison between numerical results and previous semi-empirical theories is given in Fig. 7. A reasonable agreement indicates that the present method can be used for predicting the near-field wave structure.

In additional parametric calculations for catamarans presented below, the spacing between demi-hulls s (Fig. 1) is chosen to vary between 0.5 and 2 of the demi-hull beam b. Shorter hull spacings would lead to the appearance of steep waves beyond the capabilities of the present linearized model. Also, planing multi-hulls rarely employ such narrow spacings. On the other hand, spacings above $2b$ usually result in minimal interference effects between hulls in the planing mode, as seen in Fig. 6 and discussed by others (Morabito, 2011).

Parametric calculations have been carried out for different geometrical configurations and speed regimes. Influence of hull spacings on different types of hulls, as well as hydrodynamic characteristics of a single asymmetric hull, are presented in Fig. 8. The hulls have the trim angle of 6°, the nominal wetted lengths of 3 (on the deeper side of a hull), and deadrise angles of 15°. Results are presented at two relative speeds ($Fr = 3$ and 5) for the lift slope, C_L/τ, and the center of pressure normalized by the hull beam, L_P/b. At narrow spacings between the hulls, the lift coefficients are generally higher and, as the spacing gets bigger, the changes in the lift coefficients become very small with respect to hull spacings (Fig. 8a and b). It is expected that at the wide spacings hydrodynamic parameters become less sensitive to the spacing since the hydrodynamic interference due to waves between the demi-hulls diminishes. Fig. 8a and b shows that hydrodynamic interaction is greater for the normal configuration of asymmetric hulls in comparison with the inverse setup. This is caused by more pronounced water depression (and hence bigger waves) produced by more deeply submerged

Please cite this article in press as: Bari, G.S., Matveev, K.I., Hydrodynamics of single-deadrise hulls and their catamaran configurations, International Journal of Naval Architecture and Ocean Engineering (2016), http://dx.doi.org/10.1016/j.ijnaoe.2016.11.001

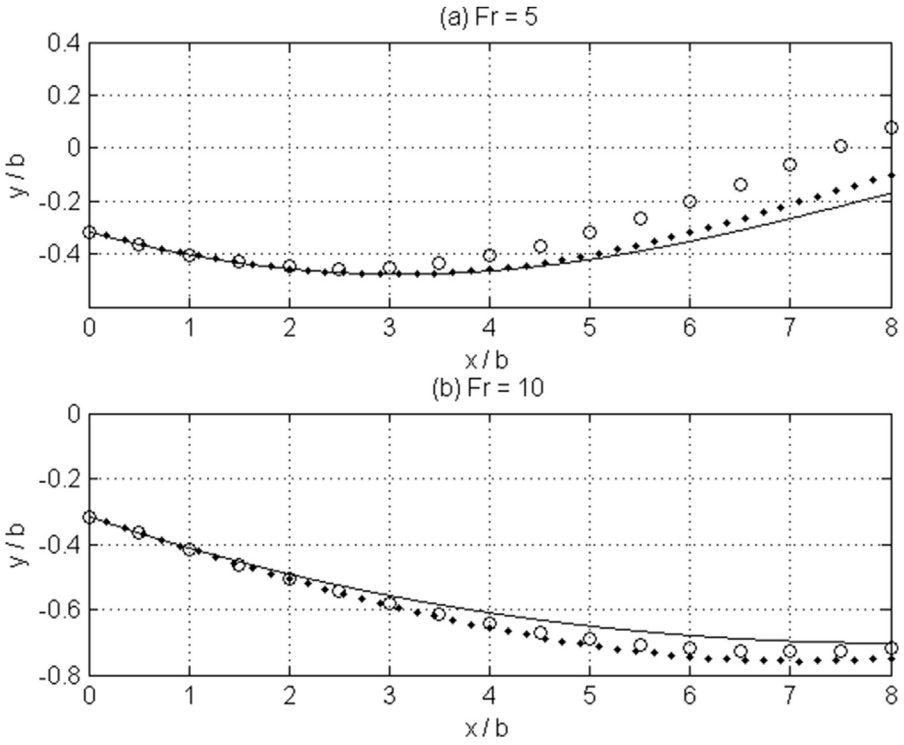

Fig. 7. Comparison of the centerline water surface profile behind a planing plate. Solid line, Payne's theory; circles, Epstein's correlation; dots, present numerical results. $x = 0$ corresponds to the plate transom.

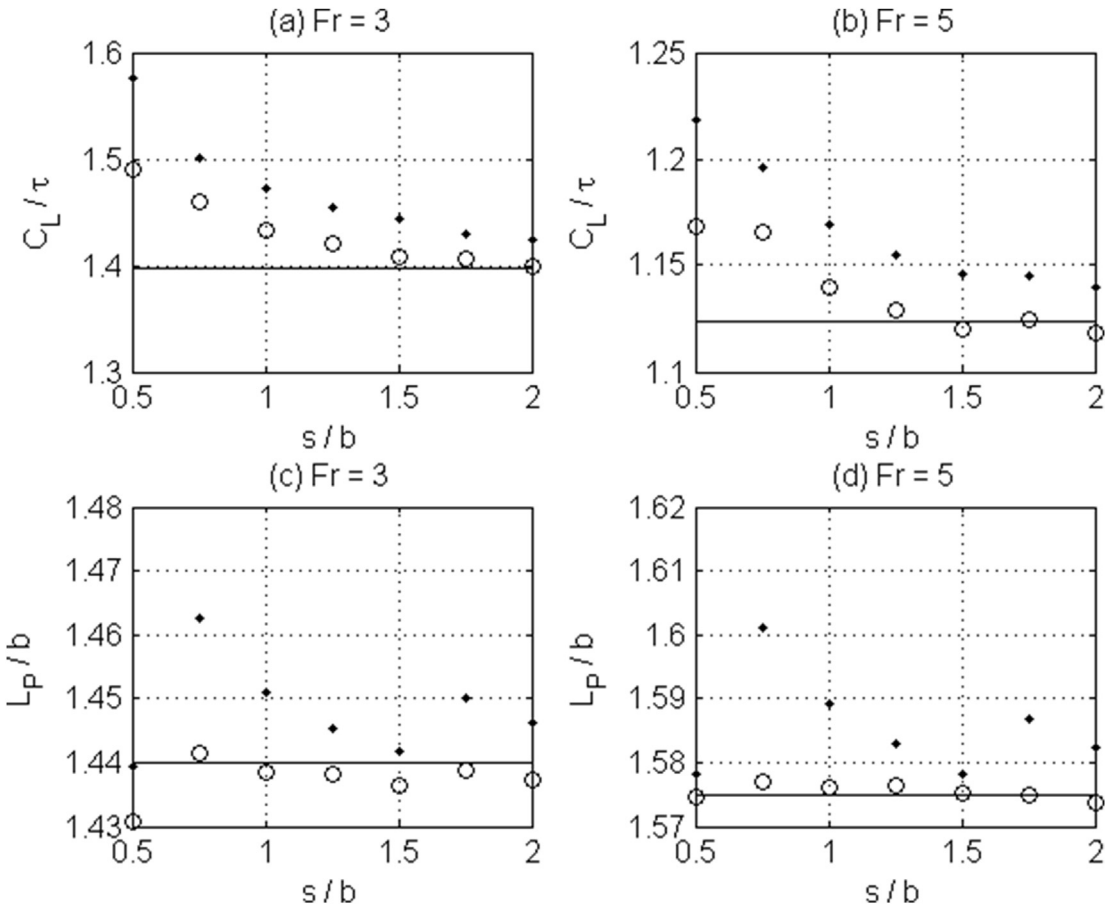

Fig. 8. Influence of hull spacing on the lift coefficient (a, b) and the center of pressure (c, d) at two Froude numbers. Dots, normal catamaran setup; circles, inverse catamaran setup; line, single asymmetric hull.

Please cite this article in press as: Bari, G.S., Matveev, K.I., Hydrodynamics of single-deadrise hulls and their catamaran configurations, International Journal of Naval Architecture and Ocean Engineering (2016), http://dx.doi.org/10.1016/j.ijnaoe.2016.11.001

longitudinal sections on the internal sides of demi-hulls in the normal arrangement. However, the difference in the lift slope between both catamaran setups, as well as single hulls, disappears at large spacings. The center of pressure demonstrates more fluctuating behavior (Fig. 8c and d), although the variations are very small. Results for L_P tend to converge at large hull spacings as well, but at very small spacings one can expect more fluctuations due to more complicated wave–hull interactions.

Fig. 9 illustrates representative wave patterns around hulls and longitudinal water surface for three configurations corresponding to Fig. 8 with Froude number of 3 and the relative hull spacing of 0.5 in the case of catamarans. For a single hull (Fig. 9a, d), the wave structure looks similar to that of a conventional planing hull demonstrating a wave hollow behind transom and formation of divergent waves (Fig. 9a). However, the water surface asymmetry can also be noticed due to a non-symmetrical hull (Fig. 9d). In the cases of catamaran setups with narrow hull spacings (Fig. 9b and c), the wave amplitudes significantly increase in the zone between hulls (Fig. 9e and f), which causes more pronounced upwash on each hull resulting in higher lift coefficients (Fig. 8a and b).

It is also important to understand how hydrodynamic characteristics change in different speed regimes. A boat with the normal demi-hull setup (Fig. 1b) and the same parameters used above (Fig. 8) has been simulated with two extreme hull spacings (0.5 and 2) in the Froude number range between 1 and 5. Results for the lift slope and the center of pressure are given in Fig. 10. For both spacings, the lift coefficient monotonically decreases with increasing Froude number, since the constant hydrostatic contribution normalized by increasing dynamic pressure declines at high *Fr*. On the other hand, the center of pressure moves forward at higher speeds because the hydrodynamic lift becomes more important and the hydrodynamic pressure is more prominent near the leading point of the wetted surface. As one can see in Fig. 10, the sensitivity to Froude number is much greater than to the hull spacing. For the narrow spacing setup the lift is greater at *Fr* above 2, but at low speeds ($Fr = 1$) the lift is nearly the same for both spacings, since the hydrostatic force is dominant.

To illustrate effects of different aspect ratio and deadrise angles of demi-hulls, calculations have been carried out for the normal twin-hull setups with $s/b = 0.5$, $\tau = 6°$, $Fr = 3$, variable deadrise angle and two nominal aspect ratios $\lambda_{nk} = L_{nk}/b$

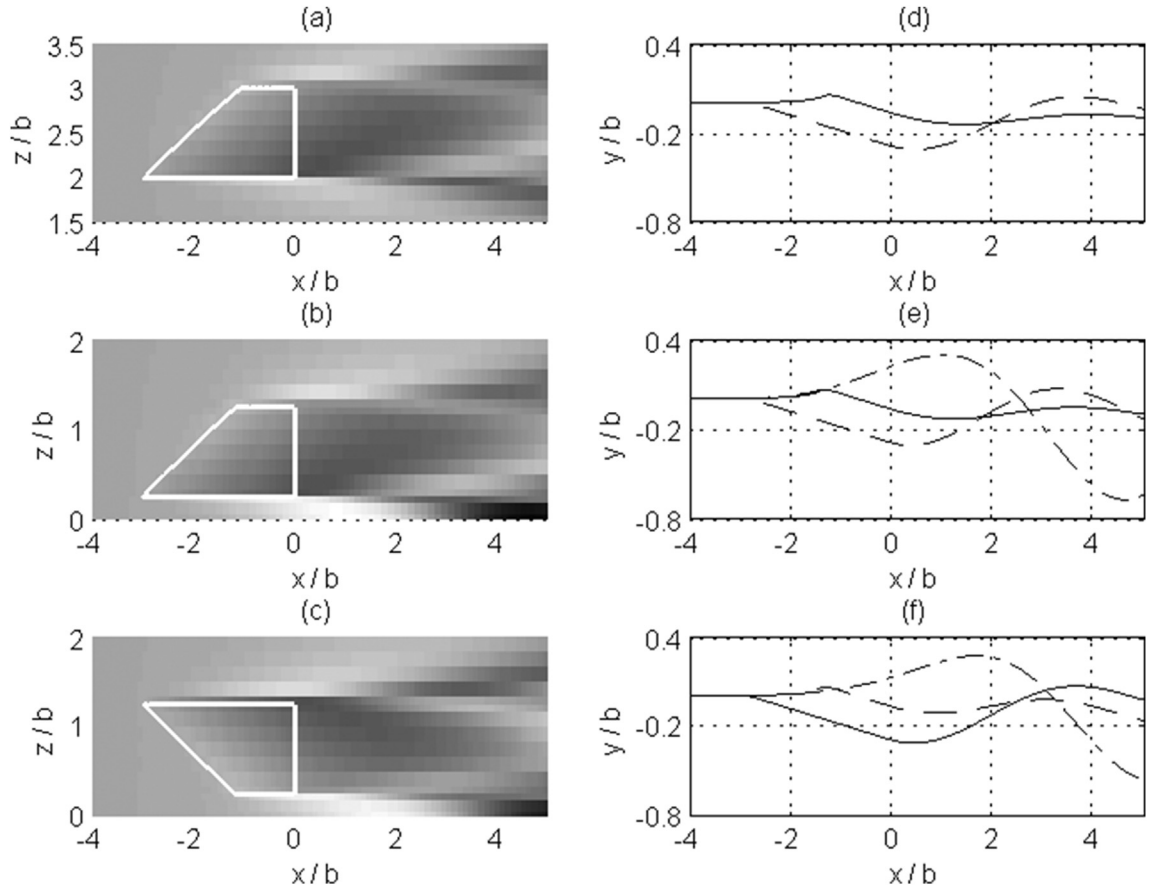

Fig. 9. (a–c) Top views of water surface contours around (a) single hull, (b) starboard demi-hull in the normal catamaran setup, and (c) similar demi-hull in the inverse setup. Brightness scales with the water surface elevation. The incident flow is directed along the x-axis. Solid white lines surround the hull pressure areas. z = 0 is the symmetry plane in (b) and (c). (d–f) Longitudinal sections of water surface elevations at 8% of the demi-hull span from the starboard side (solid line) and port side (dashed line) of the starboard demi-hull. The dash-dotted lines in (e) and (f) correspond to the catamaran centerline (z = 0).

Please cite this article in press as: Bari, G.S., Matveev, K.I., Hydrodynamics of single-deadrise hulls and their catamaran configurations, International Journal of Naval Architecture and Ocean Engineering (2016), http://dx.doi.org/10.1016/j.ijnaoe.2016.11.001

(2 and 4), where L_{nk} is the nominal wetted length (Fig. 3) at the keel section (i.e., on the port side of the starboard demi-hull in the normal catamaran setup). Results for the lift slope and the center of pressure are shown in Fig. 11. As expected, both C_L/τ and L_P/b decrease with increasing deadrise, as the hulls become less hydrodynamically efficient and the wetted areas recede toward the hull stern. The beam-based lift coefficient and the center of pressure are greater for higher aspect ratio hulls, since at a constant hull beam the pressure area increases and elongates toward the hull bow.

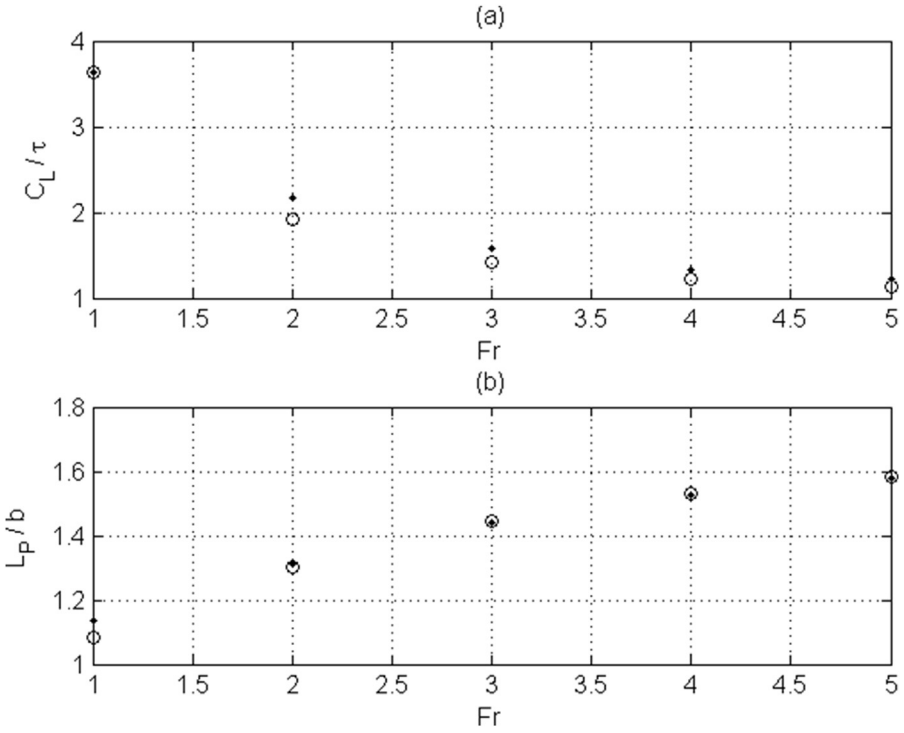

Fig. 10. Influence of Froude number on (a) lift slope and (b) center of pressure. Circles, $s/b = 2$; dots, $s/b = 0.5$.

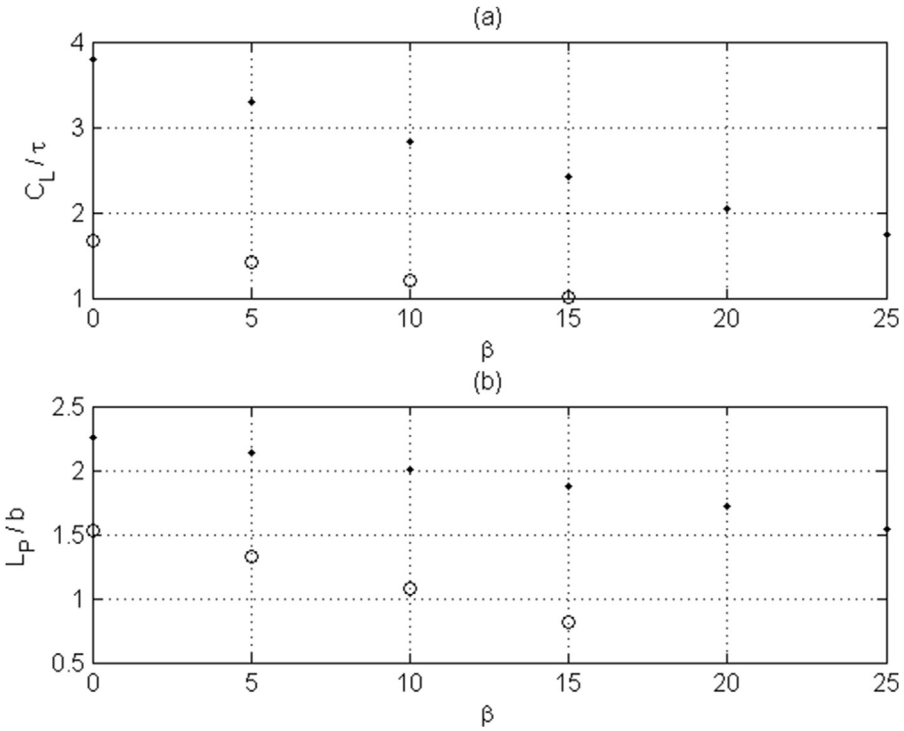

Fig. 11. Influence of the deadrise angle on (a) lift slope and (b) center of pressure. Circles, $\lambda_{nk} = 2$; dots, $\lambda_{nk} = 4$.

Please cite this article in press as: Bari, G.S., Matveev, K.I., Hydrodynamics of single-deadrise hulls and their catamaran configurations, International Journal of Naval Architecture and Ocean Engineering (2016), http://dx.doi.org/10.1016/j.ijnaoe.2016.11.001

4. Conclusions

A potential flow method has been applied in this work for modeling hydrodynamics of planing single-deadrise hulls and their catamaran setups. The model has been validated against experimental data available for single asymmetric hulls and twin-hull arrangements. Parametric calculations indicate that the lift force increases with decreasing hull spacing, and this effect is stronger for the normal twin-hull setup with deeper submergence of the internal sides of demi-hulls. The lift coefficient decreases whereas the center of pressure moves forward with increasing Froude number similar to conventional planing hulls. Higher deadrise angles lead to a reduction of the lift coefficient and aftward shift of the center of pressure.

The obtained results can assist designers of high-speed catamarans in evaluating hydrodynamic characteristics in different speed regimes and hull dimensions. The present model can be further extended to incorporate aerodynamic lift (in the tunnel between hulls) and more sophisticated hull features, including steps, variable deadrise, hydrofoils, and control surfaces.

References

Bari, G.S., Matveev, K.I., 2016. Hydrodynamic modeling of planing catamarans with symmetric hulls. Ocean Eng. 115, 60–66.
Benedict, K., Kornev, N., Meyer, M., Ebert, J., 2002. Complex mathematical model of the WIG motion including the take-off mode. Ocean Eng. 29, 315–357.
Bertram, V., 2000. Practical Ship Hydrodynamics. Butterworth-Heinemann, Oxford.
Doctors, L.J., 1974. Representation of planing surfaces by finite pressure elements. In: 5th Australian Conference on Hydraulics and Fluid Mechanics, Christchurch, New Zealand.
Epstein, L.A., 1969. Determination of the depression behind a finite-span underwater wing and gliding flat plate. In: Problems of Hydrodynamics and Continuum Mechanics. SIAM, Philadelphia, PA, pp. 220–230.
Judge, C.Q., 2013. Comparisons between prediction and experiment for lift force and heel moment for a planing hull. J. Ship Des. Prod. 29 (1), 36–46.
Kandasamy, M., Ooi, S.K., Carrica, P., Stern, F., Campana, E.F., Peri, D., Osborne, P., Cote, J., Macdonald, N., de Waal, N., 2011. CFD validation studies for a high-speed foil-assisted semi-planing catamaran. J. Mar. Sci. Technol. 16 (2), 157–167.
Knapp, R.T., Daily, J.W., Hammit, F.G., 1970. Cavitation. McGraw-Hill, New York.
Lai, C., Troesch, A.W., 1996. A vortex lattice method for high-speed planing. Int. J. Numer. Methods Fluids 22, 495–513.
Lee, T.-S., 1982. Interference factor for catamaran planing hulls. AIAA J. 20 (10), 1461–1462.
Liu, C.Y., Wang, C.T., 1979. Interference effects of catamaran planing hulls. J. Hydronautics 13 (1), 31–32.
Matveev, K.I., 2003. On the limiting parameters of artificial cavitation. Ocean Eng. 30 (9), 1179–1190.
Matveev, K.I., Ockfen, A., 2009. Modeling of hard-chine hulls in transitional and early planing regimes by hydrodynamic point sources. Int. Shipbuild. Prog. 56, 1–13.
Matveev, K.I., Miller, M.J., 2011. Air cavity with variable length under model hull. J. Eng. Marit. Environ. 225 (2), 161–169.
Matveev, K.I., 2014a. Hydrodynamic modeling of planing hulls with twist and negative deadrise. Ocean Eng. 82, 14–19.
Matveev, K.I., 2014b. Modeling of finite-span ram wings moving above water at finite Froude numbers. J. Ship Res. 58 (3), 146–156.
Migeotte, G., 2002. Design and Optimization of Hydrofoil-assisted Catamarans (Ph.D. thesis). University of Stellenbosch, Stellenbosch, South Africa.
Morabito, M.G., 2011. Experimental investigation of the lift and interference of asymmetric planing catamaran demi-hulls. In: 11th International Conference on Fast Sea Transportation. Hawaii, USA, Honolulu.
Payne, P.R., 1984. On the shape of the wake behind a planing boat. Ocean Eng. 11 (5), 513–524.
Payne, P.R., 1988. Design of High-Speed Boats: Planing. Fishergate, Annapolis, MD.
Savitsky, D., Dingee, D., 1954. Some Interference Effects between Two Flat Surfaces Planing Parallel to Each Other at High Speed. Davidson Laboratory Technical Note No. 247.
Savitsky, D., Prowse, R.E., Lueders, D.H., 1958. High-speed Hydrodynamic Characteristics of a Flat Plate and 20° Dead-rise Surface in Unsymmetrical Planing Conditions. NACA Technical Note 4187.
Savitsky, D., 1964. Hydrodynamic design of planing hulls. Mar. Technol. 1, 71–95.
Yousefi, R., Shafaghat, R., Shakeri, M., 2013. Hydrodynamic analysis techniques for high-speed planing hulls. Appl. Ocean Res. 42, 105–113.
Yousefi, R., Shafaghat, R., Shakeri, M., 2014. High-speed planing hull drag reduction using tunnels. Ocean. Eng. 84, 54–60.
Zhou, Z., 2003. A Theory and Analysis of Planing Catamarans in Calm and Rough Water (Ph.D. thesis). University of New Orleans.

Please cite this article in press as: Bari, G.S., Matveev, K.I., Hydrodynamics of single-deadrise hulls and their catamaran configurations, International Journal of Naval Architecture and Ocean Engineering (2016), http://dx.doi.org/10.1016/j.ijnaoe.2016.11.001